

Research Article

A Bright Entanglement and Squeezing Generated by an External Pumping Radiation in a Correlated Emission Laser

Chimdessa Gashu 

Department of Physics, Jimma University, P.O. Box 378, Jimma, Ethiopia

Correspondence should be addressed to Chimdessa Gashu; chimdessagashu@gmail.com

Received 21 April 2020; Revised 13 June 2020; Accepted 19 August 2020; Published 2 September 2020

Academic Editor: E. Bernabeu

Copyright © 2020 Chimdessa Gashu. This is an open access article distributed under the Creative Commons Attribution License, which permits unrestricted use, distribution, and reproduction in any medium, provided the original work is properly cited.

The quantum and statistical properties of light generated by an external classical field in a correlated emission laser with a parametric amplifier and coupled to a squeezed vacuum reservoir are investigated using the combination of the master and stochastic differential equations. First, the solutions of the cavity-mode variables and correlation properties of noise forces associated to the normal ordering are obtained. Next, applying the resulting solutions, the mean photon number of the separate cavity modes and their crosscorrelation, smallest eigenvalue of the symplectic matrix, mean photon number, intensity difference fluctuation, photon number variance, and intensity correlation are derived for the cavity-mode radiation. The entanglement produced is studied employing the logarithmic negativity criterion. It is found that pumping atoms from the lower energy state to excited state, introducing the nonlinear crystal into the cavity and coupling the system to a biased noise fluctuation, generate a bright and strong squeezing and entanglement with enhanced statistical properties although the atoms are initially in the ground state.

1. Introduction

A search for quantum systems that would generate a strongly correlated two photons is an active area of theoretical and experimental investigations [1–4]. This research interest is predominantly linked to the intuitively manageable quantum features associated to the two-photon processes. The extensively studied quantum features, which are attributed to the correlation of the two-photon, are continuous variable quantum discord, quantum steering, quadrature squeezing, and quantum entanglement [5, 6]. Moreover, a three-level cascade laser has been an interesting area of research over the years in light of its capability to produce radiations with rich varieties of the nonclassical properties [1–7]. The coherence induced between the dipole forbidden atomic transitions is accountable for the generation of quantum and statistical properties of the light in this optical device. One of the viable methods to generate correlation between the three-level cascade atoms would be pumping its top and bottom energy levels with a strong classical driving field [5, 8–10]. Such mechanism imposes a constraint on the

populations of atoms in the bottom and top levels in which transitions to and from could not be made in the electric dipole approximation scheme. The classical pumping radiation contributes to the observed nonclassical properties by facilitating atomic population transfer pathway in which the induced atomic correlation is transferred to the two-mode cavity photons.

Moreover, several authors have demonstrated that introducing a nonlinear crystal into a correlated emission laser amplifies the nonclassical properties of radiation [11–21]. These authors have used either degenerate or nondegenerate parametric amplifiers which are described based on the frequencies of the output signal and idler photons generated after the down conversion process. The correlation between the signal and idler photons leads to squeezing of 50% degree below the standard quantum limit [22]. It can also be used in such a way that the introduction of these crystals into a correlated emission laser optimizes the quantum properties of the light [23, 24]. Squeezing is a light with phase-sensitive quantum fluctuations, which, at certain phase angles, are less than those of a perfectly coherent light and vacuum state of

no field at all. In a squeezed state, the quantum noise in one quadrature is below the coherent or vacuum level at the expense of enhanced fluctuations in the conjugate quadrature, with the product of the uncertainties in the two quadratures satisfying the uncertainty relation [24]. Squeezed light has potential applications in quantum communications, detections of weak signals, and high precision measurements in atomic fountain clocks and interferometers [25, 26]. In addition, the amount of entanglement, which is a resource of tasks such as quantum memories for quantum computers [27], quantum information and communication [28], quantum dense coding [29], quantum teleportation for secure communication [30], and atom clocks and interferometers for quantum sensing and metrology [31], enhances with the parametric amplifier [32].

However, the squeezing, entanglement, and mean photon number of the cavity radiation have been found to be insignificant for the case in which all the atoms are initially prepared in the bottom level [33, 34] even in the presence of the parametric amplifier. In this situation, an external pumping radiation has been employed to further investigate the nonclassical properties of the light produced by a coherently pumped correlated emission laser whose cavity is coupled to the vacuum reservoir, in the absence of the parametric amplifier and for the case in which the atoms are initially prepared in the aforementioned manner [35]. In this work, the achievable degree of the squeezing and continuous variable entanglement of the cavity radiation have been observed to be nearly 50% below the standard quantum limit and occurred near the threshold condition. The author has mainly focused to show the possibility of entanglement and squeezing production with the classical pumping radiation disregarding their strength. On the contrary, for the quantum information processing tasks, the degree of the squeezing and entanglement must be quite robust against decoherences. Therefore, this paper is mainly concentrated to investigate the role of the nonlinear crystal and squeezed vacuum environment which may improve the amount of the nonclassical properties of the radiation generated in the proposed scheme.

In this work, the squeezing, entanglement, and photon statistics of a correlated emission laser coupled to a two-mode squeezed vacuum reservoir and containing the parametric amplifier are studied. The motivation of this work is that the parametric amplifier and squeezed vacuum reservoir could enhance the nonclassical properties of interest. Moreover, on the basis of the existing practical challenges in preparing the atoms initially in an arbitrary atomic coherence and due to the sensitivity of the quantum features to the inevitable effect decoherence from an external environment, it is supposed that the quantum system under consideration can be one of the interesting schemes in generating a significantly enhanced quantum and statistical features. In order to carry out our analyses, the master equation is derived by applying the linear and adiabatic approximations in the good cavity limit following the standard method presented in [35]. Employing the master equation, the stochastic differential equations, then the

solutions for c -number cavity-mode variables, and correlation property of the noise forces associated to the normal ordering are determined.

2. The Model

The three-level cascade atoms, which are initially prepared in a bottom level, are injected into the cavity at a constant rate and removed from the laser cavity after they spontaneously decay to the external environment. The top and bottom levels are linked by the classical driving radiation similar to the case of lasing without population inversion. Three-level atoms interact with resonant cavity modes and a nondegenerate parametric amplifier (NLC) in the laser cavity. Here, the cavity light is coupled to the squeezed vacuum environment. As it can be seen in Figure 1, the top, intermediate, and bottom levels of a three-level atom are indicated by $|l\rangle$, $|m\rangle$, and $|n\rangle$. It is assumed that transitions $|l\rangle$ to $|m\rangle$ and $|m\rangle$ to $|n\rangle$ are dipole allowed transitions with frequencies ω_l and ω_m , respectively, while transitions between levels $|l\rangle$ and $|n\rangle$ are dipole forbidden.

In the nondegenerate three-level laser, a pump mode of frequency, $\omega = \omega_l + \omega_m$, directly interacts with the nonlinear crystal inside laser cavity mirrors to produce the signal and idler photons having the same frequencies as the two dipole-allowed atomic transitions [35]. The electric dipole and rotating-wave approximations are applied to describe the down conversion process in a nonlinear crystal in the interaction picture as

$$\hat{H}_{\text{NLC}} = i\varepsilon(\hat{a}^\dagger \hat{b}^\dagger - \hat{a}\hat{b}), \quad (1)$$

in which the real constant parameter ε is proportional to the amplitude of the pump mode that drives the nonlinear crystal and \hat{a} (\hat{b}) are the annihilation operators for the two cavity modes. The master equation associated to this particular Hamiltonian is

$$\frac{d}{dt}\hat{\rho} = \varepsilon(\hat{a}^\dagger \hat{b}^\dagger \hat{\rho} - \hat{\rho} \hat{a}^\dagger \hat{b}^\dagger - \hat{a}\hat{b}\hat{\rho} + \hat{\rho}\hat{a}\hat{b}), \quad (2)$$

where $\hat{\rho}$ is the density operator for the cavity-mode radiation.

On the contrary, the interaction of a three-level atom with a two-mode cavity light can be described in the interaction picture with the electric dipole and rotating-wave approximations as

$$\hat{H}_{\text{AC}} = ig[\hat{a}^\dagger |m\rangle\langle l| + \hat{b}^\dagger |n\rangle\langle m| - \hat{a}|l\rangle\langle m| - \hat{b}|m\rangle\langle n|], \quad (3)$$

where the constant g is considered to be the same for both dipole allowed transitions for convenience.

Moreover, the interaction Hamiltonian operator describing the coupling of the dipole forbidden transition is describable in the interaction picture as

$$\hat{H}_d = i\frac{\Omega}{2}[|n\rangle\langle l| - |l\rangle\langle n|], \quad (4)$$

where Ω is the amplitude of the external pumping radiation.

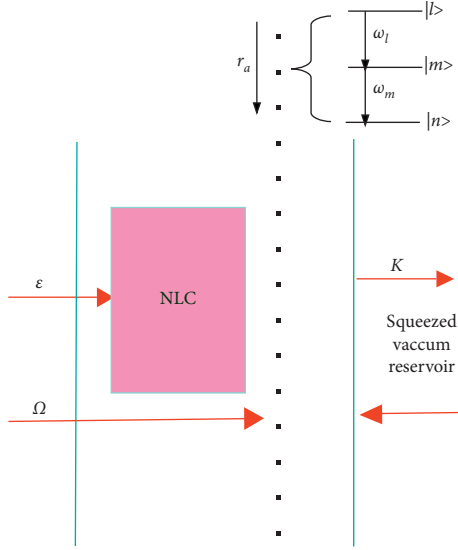


FIGURE 1: Schematic representation of a correlated emission laser with a nonlinear crystal (NLC) and coupled to a two-mode squeezed vacuum reservoir.

On the basis of equations (3) and (4), the interaction of a three-level cascade atom, whose top and bottom levels are initially prepared in the bottom level and coupled by external coherent radiation, with a two-mode cavity radiation, can be described by the interaction Hamiltonian of the form

$$\begin{aligned} \hat{H}_t = & ig \left[\hat{a}^\dagger |m\rangle \langle l| - \hat{a} |l\rangle \langle m| + \hat{b}^\dagger |n\rangle \langle m| - \hat{b} |m\rangle \langle n| \right] \\ & + i \frac{\Omega}{2} [|n\rangle \langle l| - |l\rangle \langle n|]. \end{aligned} \quad (5)$$

Moreover, in this work, the three-level cascade atoms are assumed to be initially prepared in the bottom (lower energy) level which corresponds to the absence of coherence among the noninteracting atoms. These atoms are injected into a cavity at constant rate r_a and removed after some time τ . The spontaneous decay rate γ is assumed to be the same for each level. In the good cavity limit, $\gamma \gg \kappa$, where κ is the cavity damping constant, the cavity-mode variables change slowly compared with the atomic variables. Hence, the atomic variables will reach the steady state in a relatively short time. Therefore, it is quite justifiable to remove the atomic variables adiabatically. In addition, the coupling constant is taken to be small, and we apply the linear approximation that amounts to removing higher order terms in g . The linear approximation preserves the quantum properties we seek to study as these properties are attributed to the classical driving radiation that couples the top and bottom states. Hence, using equations (2) and (5) along with the linear and adiabatic approximations in the good cavity limit, the equation of evolution of the density operator for the cavity modes coupled to a two-mode squeezed vacuum reservoir is found to be

$$\begin{aligned} \frac{d\hat{\rho}}{dt} = & \varepsilon \left[\hat{\rho} \hat{a} \hat{b} - \hat{a} \hat{b} \hat{\rho} + \hat{a}^\dagger \hat{b}^\dagger \hat{\rho} - \hat{\rho} \hat{a}^\dagger \hat{b}^\dagger \right], \\ & + \frac{\kappa}{2} (N + 1) \left[2\hat{a} \hat{\rho} \hat{a}^\dagger - \hat{a}^\dagger \hat{a} \hat{\rho} - \hat{\rho} \hat{a}^\dagger \hat{a} \right], \\ & + \frac{1}{2} \left(\frac{3A\zeta^2}{2\chi} + \kappa N \right) \left[2\hat{a}^\dagger \hat{\rho} \hat{a} - \hat{a} \hat{a}^\dagger \hat{\rho} - \hat{\rho} \hat{a} \hat{a}^\dagger \right], \\ & + \frac{1}{2} \left(\frac{A(4 + \zeta^2)}{2\chi} + \kappa(N + 1) \right) \left[2\hat{b} \hat{\rho} \hat{b}^\dagger - \hat{b}^\dagger \hat{b} \hat{\rho} - \hat{\rho} \hat{b}^\dagger \hat{b} \right], \\ & + \frac{\kappa}{2} N \left[2\hat{b}^\dagger \hat{\rho} \hat{b} - \hat{b} \hat{b}^\dagger \hat{\rho} - \hat{\rho} \hat{b} \hat{b}^\dagger \right], \\ & - \frac{A\zeta(4 + \zeta^2)}{\chi} \left[\hat{a} \hat{b} \hat{\rho} - \hat{a}^\dagger \hat{\rho} \hat{b}^\dagger + \hat{\rho} \hat{b}^\dagger \hat{a}^\dagger - \hat{b} \hat{\rho} \hat{a} \right], \\ & + \frac{A\zeta(\zeta^2 - 2)}{\chi} \left[\hat{b}^\dagger \hat{a}^\dagger \hat{\rho} - \hat{a}^\dagger \hat{\rho} \hat{b}^\dagger + \hat{\rho} \hat{a} \hat{b} - \hat{b} \hat{\rho} \hat{a} \right], \\ & + \kappa M \left[\hat{a}^\dagger \hat{b}^\dagger \hat{\rho} + \hat{\rho} \hat{a}^\dagger \hat{b}^\dagger - \hat{b}^\dagger \hat{\rho} \hat{a}^\dagger - \hat{a}^\dagger \hat{\rho} \hat{b}^\dagger \right], \\ & + \kappa M \left[\hat{\rho} \hat{a} \hat{b} + \hat{a} \hat{b} \hat{\rho} - \hat{b} \hat{\rho} \hat{a} - \hat{a} \hat{\rho} \hat{b} \right], \end{aligned} \quad (6)$$

in which $\chi = 2(1 + \zeta^2)(4 + \zeta^2)$. Setting $r = \varepsilon = 0$ in equation (6) reproduces the master equation obtained in [34].

The result presented in equation (6) indicates the stochastic master equation which contains all necessary information about the dynamics of the system incorporating the effect of the huge external environment. On the contrary, the amplitude of the classical driving radiation is determined by $\zeta = (\Omega/\gamma)$ since γ is fixed. Besides, $A = (2r_a g^2/\gamma^2)$ indicates the linear gain coefficient. N and M account for the external environment on the quantum optical system. The constants $N = \sinh^2(r)$ and $M = \sinh(r)\cosh(r)$, in which r is the squeeze parameter.

3. Stochastic Differential Equations

In this section, we apply equation (6) and the relation $(d/dt)\langle \hat{A} \rangle = \text{Tr}((d\hat{\rho}/dt)\hat{A})$ to obtain the time development of the cavity-mode variables as follows:

$$\frac{d}{dt} \langle \hat{a} \rangle = -\mu_+ \langle \hat{a} \rangle - \eta_+ \langle \hat{b}^\dagger \rangle, \quad (7)$$

$$\frac{d}{dt} \langle \hat{b} \rangle = -\mu_- \langle \hat{b} \rangle - \eta_- \langle \hat{a}^\dagger \rangle, \quad (8)$$

$$\frac{d}{dt} \langle \hat{a}^2 \rangle = -2\mu_+ \langle \hat{a}^2 \rangle - 2\eta_+ \langle \hat{b}^\dagger \hat{a} \rangle, \quad (9)$$

$$\frac{d}{dt} \langle \hat{b}^2 \rangle = -2\mu_- \langle \hat{b}^2 \rangle - 2\eta_- \langle \hat{a}^\dagger \hat{b} \rangle, \quad (10)$$

$$\frac{d}{dt} \langle \hat{a}^\dagger \hat{a} \rangle = -2\mu_+ \langle \hat{a}^\dagger \hat{a} \rangle - \eta_+ \left[\langle \hat{a}^\dagger \hat{b}^\dagger \rangle + \langle \hat{a} \hat{b} \rangle \right] + \frac{3A\zeta^2}{2\chi} + \kappa N, \quad (11)$$

$$\frac{d}{dt} \langle \hat{b}^\dagger \hat{b} \rangle = -2\mu_- \langle \hat{b}^\dagger \hat{b} \rangle - \eta_- \left[\langle \hat{b}^\dagger \hat{a}^\dagger \rangle + \langle \hat{a} \hat{b} \rangle \right] + \kappa N, \quad (12)$$

$$\frac{d}{dt} \langle \hat{a}^\dagger \hat{b} \rangle = -(\mu_+ + \mu_-) \langle \hat{a}^\dagger \hat{b} \rangle - \eta_- \langle \hat{a}^{\dagger 2} \rangle - \eta_+ \langle \hat{b}^2 \rangle, \quad (13)$$

$$\begin{aligned} \frac{d}{dt} \langle \hat{a} \hat{b} \rangle = & -(\mu_+ + \mu_-) \langle \hat{a} \hat{b} \rangle - \eta_- \langle \hat{a}^\dagger \hat{a} \rangle - \eta_+ \langle \hat{b}^\dagger \hat{b} \rangle \\ & - \left[\frac{A\Sigma}{\chi} - (\varepsilon + \kappa M) \right], \end{aligned} \quad (14)$$

where

$$\mu_\pm = \frac{\kappa}{2} - \frac{A}{\chi} \left[(\zeta^2 - 2) \pm 2(1 + \zeta^2) \right], \quad (15)$$

$$\eta_\pm = -\varepsilon + \frac{A}{\chi} \left[-\zeta(1 + \zeta^2) \mp 3\zeta \right]. \quad (16)$$

We see that the cavity-mode operators in equations (7)–(14) are put in the normal order. Thus, they can be expressed in terms of the c -number variables associated to them. It is thus possible to write equations (7)–(8) as

$$\frac{d}{dt} \alpha(t) = -\mu_+ \alpha(t) - \eta_+ \beta^*(t) + f_\alpha(t), \quad (17)$$

$$\frac{d}{dt} \beta(t) = -\mu_- \beta(t) - \eta_- \alpha^*(t) + f_\beta(t), \quad (18)$$

where $f_\alpha(t)$ and $f_\beta(t)$ are the noise forces for which we find the following correlation properties:

$$\langle f_\alpha(t) \rangle = \langle f_\beta(t) \rangle = \langle f_\alpha(t) f_\beta^*(t') \rangle = 0, \quad (19)$$

$$\langle f_\beta(t) f_\beta(t') \rangle = \langle f_\alpha(t') f_\alpha(t) \rangle = 0, \quad (20)$$

$$\langle f_\alpha^*(t) f_\alpha(t') \rangle = \left(\frac{3A\zeta^2}{2\chi} + \kappa N \right) \delta(t - t'), \quad (21)$$

$$\langle f_\beta^*(t) f_\beta(t') \rangle = \kappa N \delta(t - t'), \quad (22)$$

$$\langle f_\alpha(t) f_\beta(t') \rangle = - \left[\frac{A\Sigma}{\chi} - (\varepsilon + \kappa M) \right] \delta(t - t'), \quad (23)$$

with $\Sigma = \zeta(2 - \zeta^2)$. We observe that the sources of the noise forces are the external radiations.

The solutions of the cavity-modes variables, following the procedure outlined in [10, 21, 24], are given by

$$\alpha(t) = A_+(t)\alpha(0) + B_+(t)\beta^*(0) + F_+(t) + G_+(t), \quad (24)$$

$$\beta(t) = A_-(t)\beta(0) + B_-(t)\alpha^*(0) + F_-(t) + G_-(t), \quad (25)$$

in which

$$A_\pm(t) = \frac{1}{2} \left[(1 \pm p)e^{-\nu_\pm t} + (1 \mp p)e^{-\nu_\mp t} \right], \quad (26)$$

$$B_\pm(t) = \frac{q_\pm}{2} \left[e^{-\nu_\pm t} - e^{-\nu_\mp t} \right], \quad (27)$$

$$F_+(t) = \frac{1}{2} \int_0^t \left[(1+p)e^{-\nu_-(t-t')} + (1-p)e^{-\nu_+(t-t')} \right] \times f_\alpha(t') dt', \quad (28)$$

$$F_-(t) = \frac{1}{2} \int_0^t \left[(1-p)e^{-\nu_-(t-t')} + (1+p)e^{-\nu_+(t-t')} \right] \times f_\beta(t') dt', \quad (29)$$

$$G_+(t) = \frac{q_+}{2} \int_0^t \left[e^{-\nu_+(t-t')} - e^{-\nu_-(t-t')} \right] f_\beta^*(t') dt', \quad (30)$$

$$G_-(t) = \frac{q_-}{2} \int_0^t \left[e^{-\nu_+(t-t')} - e^{-\nu_-(t-t')} \right] f_\alpha^*(t') dt', \quad (31)$$

with

$$p = \frac{1 + \zeta^2}{\Upsilon}, \quad (32)$$

$$q_\pm = \frac{-[\zeta(1 + \zeta^2) + (64\varepsilon\chi/A)] \mp 3\zeta}{2\Upsilon}, \quad (33)$$

$$\nu_\pm = \frac{\kappa}{2} - \frac{A}{4\chi} \left[(\zeta^2 - 2) \mp \Upsilon \right], \quad (34)$$

$$\Upsilon = \left[(1 + \zeta^2)^2 + \left(\frac{\zeta}{2}(1 + \zeta^2) + \frac{2\varepsilon\chi}{A} \right)^2 - \frac{9\zeta^2}{4} \right]^{1/2}. \quad (35)$$

Now, supposing the initial states of the cavity modes to be in a vacuum state, in view of the fact that the noise force at some time t does not affect the cavity-mode variables at earlier times and with the help of equations (19)–(25), the various expectation values of the cavity-mode variables are found to be

$$\langle \alpha^2 \rangle = \langle \beta^2 \rangle = \langle \alpha^* \beta \rangle = 0, \quad (36)$$

$$\begin{aligned} \langle \alpha^* \alpha \rangle = & \left[\frac{((3A\zeta^2/2\chi) + \kappa N)(1-p)^2 + \kappa N q_+^2}{8\nu_+} \right. \\ & - \left[\frac{((A\Sigma/2\chi) - 2(\varepsilon + \kappa M))q_+(1-p)}{8\nu_+} \right. \\ & + \left[\frac{((3A\zeta^2/2\chi) + \kappa N)(1+p)^2 + \kappa N q_+^2}{8\nu_-} \right. \\ & + \left[\frac{((A\Sigma/2\chi) - 2(\varepsilon + \kappa M))q_+(1+p)}{8\nu_-} \right. \\ & + \left[\frac{((3A\zeta^2/2\chi) + \kappa N)(1-p^2) - \kappa N q_+^2}{2(\nu_+ + \nu_-)} \right. \\ & \left. \left. - \left[\frac{((A\Sigma/2\chi) - 2(\varepsilon + \kappa M))q_+ p}{2(\nu_+ + \nu_-)} \right] \right], \end{aligned} \quad (37)$$

$$\begin{aligned}
\langle \beta^* \beta \rangle = & \left[\frac{((3A\zeta^2/2\chi) + \kappa N)q_-^2 + \kappa N(1+p)^2}{8\nu_+} \right], \\
& - \left[\frac{((A\Sigma/2\chi) - 2(\varepsilon + \kappa M))q_-(1+p)}{8\nu_+} \right], \\
& + \left[\frac{((3A\zeta^2/2\chi) + \kappa N)q_-^2 + \kappa N(1-p)^2}{8\nu_-} \right], \\
& + \left[\frac{((A\Sigma/2\chi) - 2(\varepsilon + \kappa M))q_-(1-p)}{8\nu_-} \right], \\
& - \left[\frac{((3A\zeta^2/2\chi) + \kappa N)q_-^2 - \kappa N(1-p^2)}{2(\nu_+ + \nu_-)} \right], \\
& - \left[\frac{((A\Sigma/2\chi) - 2(\varepsilon + \kappa M))q_-p}{2(\nu_+ + \nu_-)} \right],
\end{aligned} \tag{38}$$

$$\begin{aligned}
\langle \alpha \beta \rangle = & \left[\frac{((3A\zeta^2/2\chi) + \kappa N)q_-(1-p) + \kappa Nq_+(1+p)}{8\nu_+} \right], \\
& - \left[\frac{((3A\zeta^2/2\chi) + \kappa N)q_-(1+p) + \kappa Nq_+(1-p)}{8\nu_-} \right], \\
& - \left[\frac{((A\Sigma/\chi) - (\varepsilon + \kappa M))(1-p^2 + q_-q_+)}{8\nu_+} \right], \\
& - \left[\frac{((A\Sigma/\chi) - (\varepsilon + \kappa M))(1-p^2 + q_-q_+)}{8\nu_-} \right], \\
& + \left[\frac{((3A\zeta^2/2\chi) + \kappa N)q_-p - \kappa Nq_+p}{2(\nu_+ + \nu_-)} \right], \\
& - \left[\frac{((A\Sigma/\chi) - (\varepsilon + \kappa M))(1+p^2 - q_-q_+)}{2(\nu_+ + \nu_-)} \right].
\end{aligned} \tag{39}$$

The result in equation (36), $\langle \alpha^2 \rangle = \langle \beta^2 \rangle = 0$, indicates the absence of intercorrelation interactions among the three-level atoms since they are assumed to leave the cavity within a short time [8]. The steady state mean photon number of the cavity modes a and b are given in equations (37)-(38). On the contrary, we present in equation (39) the correlation between the cavity modes a and b , and the nonclassical properties of the cavity radiation are attributed to this term [10]. One can easily verify that the quantities involved in equations (36)–(39) are real variables.

4. Quadrature Squeezing

In this section, we proceed to study the squeezing of the radiation produced by the proposed scheme. The intracavity squeezing of a two-mode cavity radiation can be studied by the phase and amplitude quadrature operators constructed from the separate cavity-mode operators, \hat{a} and \hat{b} as

$$\hat{c}_+ = (\hat{c}^\dagger + \hat{c}), \tag{40}$$

$$\hat{c}_- = i(\hat{c}^\dagger - \hat{c}), \tag{41}$$

where $\hat{c} = ((\hat{a} + \hat{b})/\sqrt{2})$. Now, with the help of the commutation relation $[\hat{c}, \hat{c}^\dagger] = 1$, the quadrature operators satisfy the uncertainty relation:

$$[\hat{c}_+, \hat{c}_-] = 2i. \tag{42}$$

The uncertainty relation of the two noncommuting operators can be described in the form $\Delta c_+^2 \Delta c_-^2 \geq (1/4)|[\hat{c}_+, \hat{c}_-]|^2$. We next seek to obtain the fluctuations in the quadrature operators. The fluctuations of the quadrature operators are highly important in identifying the states of the radiation fields. For instance, for coherent fields, the variances of both phase and amplitude quadrature operators are equally balanced and exactly unity. On the contrary, for thermal states, the variances of both operators must exceed unity. A two-mode radiation is said to be in a squeezed state if either $\Delta c_+^2 < 1$ or $\Delta c_-^2 < 1$ such that $\Delta c_+ \Delta c_- \geq 1$ [23, 35]. Therefore, we now proceed to find the fluctuations of these quadrature operators which are given by

$$\Delta c_\pm^2 = \langle \hat{c}_\pm^2 \rangle - \langle \hat{c}_\pm \rangle^2. \tag{43}$$

Using equations (40)-(41), equation (43) in terms of the c -number variables associated to the normal order turns out to be

$$\Delta c_\pm^2 = 1 \pm [\langle \hat{c}^{\dagger 2} \rangle \pm 2\langle \hat{c}^\dagger \hat{c} \rangle + \langle \hat{c}^2 \rangle - (\langle \hat{c}^\dagger \rangle^2 \pm 2\langle \hat{c}^\dagger \rangle \langle \hat{c} \rangle + \langle \hat{c} \rangle^2)], \tag{44}$$

which can be put in a more convenient form:

$$\Delta c_\pm^2 = 1 \pm [\langle (\gamma^* \pm \gamma)^2 \rangle - \langle (\gamma^* \pm \gamma) \rangle^2]. \tag{45}$$

Here, $\gamma = (1/\sqrt{2})(\alpha + \beta)$ and with the help of which equation (45) could be describable in the following form:

$$\Delta c_\pm^2 = 1 + [\langle \alpha^* \alpha \rangle + \langle \beta^* \beta \rangle + \langle \alpha^* \beta \rangle + \langle \beta^* \alpha \rangle \pm \frac{1}{2}(\langle \alpha^{*2} \rangle + 2\langle \alpha^* \beta^* \rangle + \langle \beta^{*2} \rangle + \langle \alpha^2 \rangle + 2\langle \alpha \beta \rangle + \langle \beta^2 \rangle)]. \tag{46}$$

Now, employing equations (36)–(39), one can easily find that

$$\begin{aligned}
\Delta c_{\pm}^2 = & 1 + \left[\frac{A}{4\chi} \left(\frac{3\zeta^2}{4} \mp \frac{\Sigma}{4} \right) + (\kappa N \pm (\varepsilon + \kappa M)) \right], \\
& \times \left[\frac{\nu_+^2 + \nu_-^2 + 6\nu_+\nu_-}{4\nu_+\nu_-(\nu_+ + \nu_-)} \right] + \left[\left(\frac{3A\zeta^2}{2\chi} + \kappa N \right), \right. \\
& \times (p^2 + q_-^2 \mp 2q_-p) + \kappa N (p^2 + q_+^2 \pm 2q_+p), \\
& \left. + \left(\frac{A\Sigma}{32\chi} - 2(\varepsilon + \kappa M) \right) [p(q_+ - q_-) \pm (p^2 - q_-q_+)] \right], \\
& \times \left[\frac{\nu_+^2 + \nu_-^2 - 2\nu_+\nu_-}{4\nu_+\nu_-(\nu_+ + \nu_-)} \right] + \left[\left(\frac{3A\zeta^2}{2\chi} + \kappa N \right) (p \mp q_-), \right. \\
& \left. - \kappa N (p \pm q_+) + \left(\frac{A\Sigma}{16\chi} - (\varepsilon + \kappa M) \right) (q_+ + q_-) \right], \\
& \times \left[\frac{\nu_+ - \nu_-}{4\nu_+\nu_-} \right].
\end{aligned} \tag{47}$$

The result in equation (47) represents the steady state expressions of the phase and amplitude quadrature squeezing Δc_{\pm}^2 and the squeezing occurs in the phase (momentum-like) quadrature operator.

The threshold condition for the system under consideration is described as

$$\nu_{\pm} = 0. \tag{48}$$

Next, the explicit dependence of the squeezing on the parametric amplifier, and squeeze parameter is investigated. Since the squeezing occurs in Δc_{\pm}^2 , we plot Δc_{\pm}^2 versus the amplitude of the coherent radiation by manipulating the rest parameters, ε and r .

It is shown in Figure 2 that it is possible to produce a strong squeezed light by altering the amplitude of the pump mode that interacts with the parametric amplifier which is restricted by the steady state condition given in equation (48). It is important to mention that the degree of squeezing predicted here is by far more amplified compared with the results reported in the previous works [4, 6, 7, 9, 10, 21]. Moreover, in the absence of the parametric amplifier and injected squeezed light, the squeezing has not been demonstrated for the atoms initially prepared in the bottom level (absence of atomic coherence) [10], whereas a very weak entangled and squeezed light could be detected in the presence of the parametric amplifier [21, 33, 36]. Moreover, it is clearly indicated in Figure 3 that a strong phase squeezing could be occurred by coupling the system of interest with the squeezed vacuum environment. The cavity radiation is found to exhibit squeezing for all parameters under consideration regardless of the observed feature at the threshold. Moreover, critical observation reveals that the variation in the degree of squeezing increases with the squeeze parameter. Such property occurs due to the fact that the more the squeeze

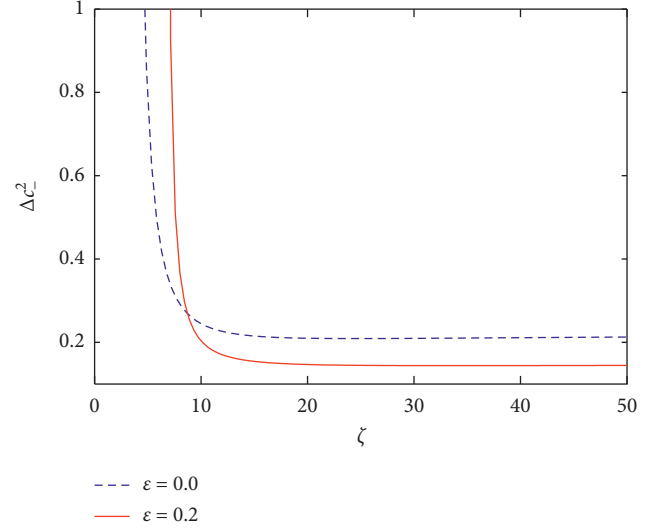


FIGURE 2: Plots of the minus quadrature variance (equation (47)) versus ζ for $\kappa = 0.8$, $A = 2.5$, and $r = 0.75$ and for different values of ε .

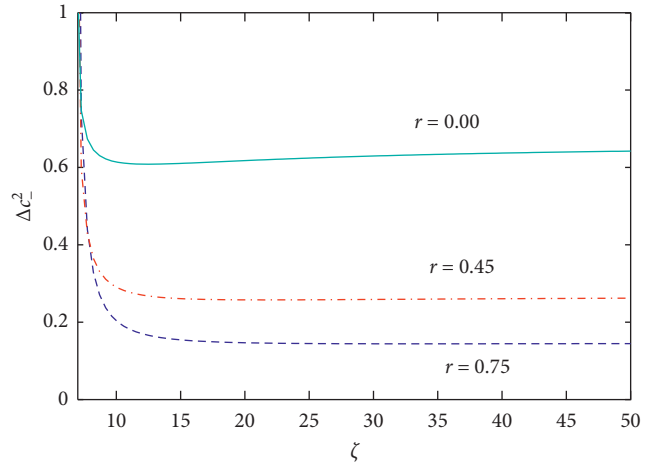


FIGURE 3: Plots of the minus quadrature variance (equation (47)) versus ζ for $\kappa = 0.8$, $A = 2.5$, and $\varepsilon = 0.20$ and for different values of r .

parameter is enhanced, the more the cavity light is dominated by the external environment. Moreover, it is found that there is no limitation imposed on the value of ζ by the steady state condition provided that the rate of atomic injection is constant. Hence, it can be argued that a squeezing of almost constant strength, over a wide range of the classical driving radiation, can be produced with the help of an external pumping radiation. This principle can also be applied to amplify the entanglement in the quantum system [8].

5. Entanglement Quantification

In this section, the entanglement of the generated radiation applying the logarithmic negativity, which is introduced in [37] for the two-mode-cavity radiation, is investigated. The

preparation and manipulation of these entangled states that have nonclassical and nonlocal properties lead to a better understanding of the basic quantum principles [10]. Nowadays, a lot of criteria have been developed to measure, detect, and manipulate the entanglement generated by various quantum optical devices. Here, we employ logarithmic negativity criterion to quantify the amount of entanglement exhibited by the correlation emission laser whose cavity contains a nonlinear crystal and the external environment is the squeezed vacuum reservoir. Logarithmic negativity is one of the relevant methods depicting the presence of entanglement for two-mode continuous variables and defined as

$$E_N = \max[0, -\log_2 V_s], \quad (49)$$

where V_s represents the smallest eigenvalue of the symplectic matrix. The entanglement is realized for positive E_N within the region of the lowest eigenvalue of covariance matrix $V_s < 1$ [8, 37, 38]. Moreover, the smallest possible eigenvalue of the symplectic spectrum of the covariance matrix of the partially transposed density operator is [8, 37]

$$V_s = \left(\frac{\bar{\zeta} - (\bar{\zeta}^2 - 4\det\Gamma)^{(1/2)}}{2} \right)^{(1/2)}, \quad (50)$$

where the invariant $\bar{\zeta}$ and matrix Γ are, respectively, denoted as

$$\bar{\zeta} = \det\mathbb{K}_1 + \det\mathbb{K}_2 - 2\det\mathbb{K}_{12}, \quad (51)$$

$$\Gamma = \begin{pmatrix} \mathbb{K}_1 & \mathbb{K}_{12} \\ \mathbb{K}_{12}^T & \mathbb{K}_2 \end{pmatrix}, \quad (52)$$

in which \mathbb{K}_1 and \mathbb{K}_2 are the covariance matrices describing each mode separately while \mathbb{K}_{12} are the intermodal correlations. The elements of the matrix in equation (52) can be obtained from the relation [37]

$$\Gamma_{ij} = 0.5\langle \hat{d}_i \hat{d}_j + \hat{d}_j \hat{d}_i \rangle - \langle \hat{d}_i \rangle \langle \hat{d}_j \rangle, \quad (53)$$

in which $i, j = 1, 2, 3, 4$. The quadrature operators are defined as $\hat{d}_1 = \hat{a} + \hat{a}^\dagger$, $\hat{d}_2 = i(\hat{a}^\dagger - \hat{a})$, $\hat{d}_3 = \hat{a} + \hat{a}^\dagger$, and $\hat{d}_4 = i(\hat{b}^\dagger - \hat{b})$.

It is not difficult to find the extended covariance matrix in terms of the c -number variables associated with the normal ordering to take the form

$$\Gamma = \begin{pmatrix} \Lambda & 0 & \lambda & 0 \\ 0 & \Lambda & 0 & -\lambda \\ \lambda & 0 & \Delta & 0 \\ 0 & -\lambda & 0 & \Delta \end{pmatrix}, \quad (54)$$

where $\Lambda = 2\langle \alpha^* \alpha \rangle + 1$, $\lambda = 2\langle \alpha \beta \rangle$, and $\Delta = 2\langle \beta^* \beta \rangle + 1$ are c -number variables associated with the normal ordering.

Next, on account of equations (52)–(54), one can readily show that

$$\det\Gamma = \left[\sqrt{\det\mathbb{K}_1 \det\mathbb{K}_2} - \sqrt{\det\mathbb{K}_{12}^T \det\mathbb{K}_{12}} \right]^2, \quad (55)$$

where $\det\mathbb{K}_1 = \Lambda^2$, $\det\mathbb{K}_2 = \Delta^2$, and $\det\mathbb{K}_{12} = -\lambda^2$.

We now investigate the variation of the entanglement of the cavity radiation with the amplitude of the parametric amplifier and squeeze parameter. To this end, we plot V_s versus the amplitude of the classical pumping radiation by alternatively altering and fixing the values ε and r at which the maximum degree of entanglement occurs in the previous plots.

It is not difficult to note in Figure 4 that the degree of entanglement for the quantum system under consideration can be enhanced with the amplitude of the parametric amplifier. In addition to this, it is found that the effect of the parametric amplifier in this case can provide a significant change in the degree of entanglement for $\zeta \geq 10$. The degree of entanglement at the threshold is in general weak since the classical driving radiation does not build a strong enough correlation between the two-cavity modes' radiation in this case [32]. Moreover, critical observation reveals ranges of ζ , for which the entanglement occurs, increases with the amplitude of the parametric amplifier. Particularly, the degree of entanglement is 80% for $\varepsilon = 0.00$ and $\zeta = 23.42$ and 86% for $\varepsilon = 0.20$ and $\zeta = 36$.

Moreover, we plot in Figure 5 to get insight on the influence of the squeezed vacuum environment on the smallest possible eigenvalue of the symplectic matrix and hence on the entanglement of the two-mode radiation for fixed ε . The smallest eigenvalue of the symplectic matrix is less than one $V_s < 1$ for all parameters under consideration indicating that the cavity radiation is entangled. The squeeze parameter enhances the achievable degree of entanglement from 40% for $r = 0$ to 85.6% for $r = 0.75$.

6. Photon Statistics

6.1. Mean Photon Number. In this section, we investigate the intensity of the cavity light. In order to get insight about the intensity of the generated light and its relation with the other nonclassical properties, it is worthwhile to study the mean number of photon of the two-mode cavity radiation. In terms of the annihilation operator of the cavity radiation, the mean photon number of the cavity light can be defined as

$$\bar{N} = \langle \hat{c}^\dagger \hat{c} \rangle. \quad (56)$$

Equation (56), in terms of c -number variables associated with the normal ordering, could be put as

$$\bar{N} = \frac{1}{2} [\langle \alpha^* \alpha \rangle + \langle \beta^* \beta \rangle]. \quad (57)$$

Equation (57) represents the mean number of photon pairs of the system.

We next investigate the variation of the mean photon number of the system, equation (57) with the squeeze parameter and parametric amplifier, and compare the brightness, squeezing, and entanglement of the cavity radiation.

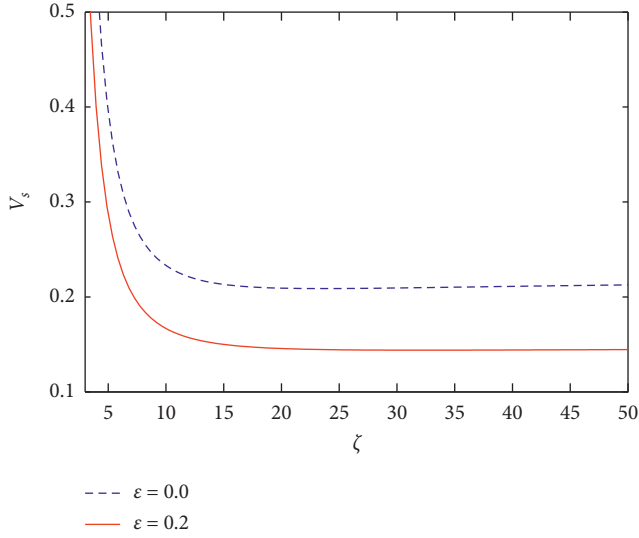


FIGURE 4: Plots of V_s (equation (26)) versus ζ for $\kappa = 0.8$, $r = 0.75$, and $A = 2.5$ and for different values of ε .

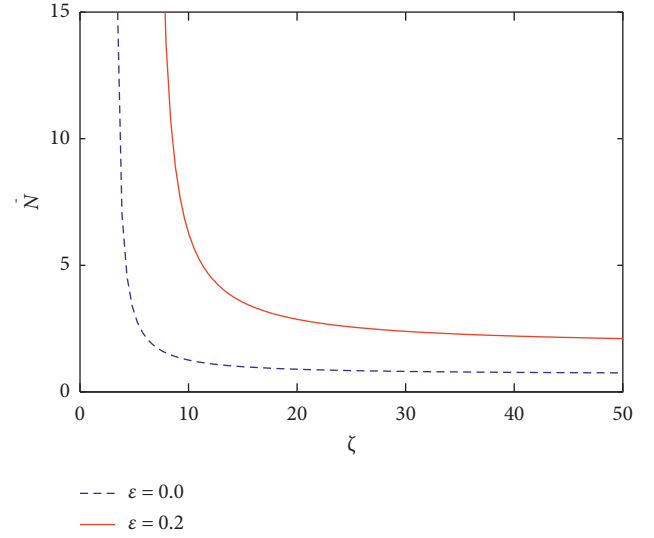


FIGURE 6: Plots of the steady state mean photon number (equation (57)) versus ζ for $\kappa = 0.8$, $r = 0.75$, and $A = 2.50$ and for different values of ε .

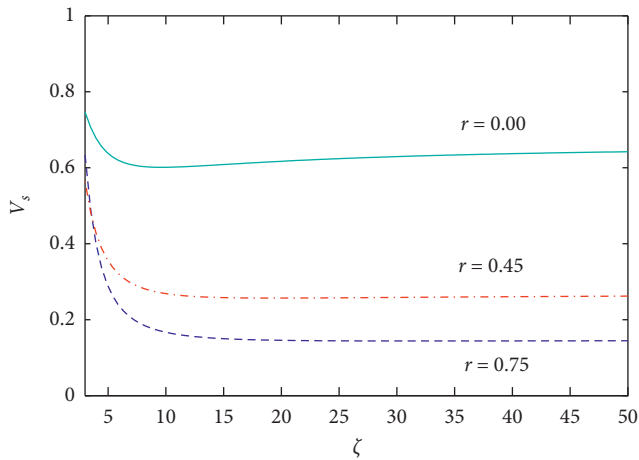


FIGURE 5: Plots of V_s (equation (26)) versus ζ for $\kappa = 0.8$, $\varepsilon = 0.20$, and $A = 2.5$ and for different values of r .

The parametric amplifier and squeeze parameter enhance the mean photon number of the cavity light, as reflected in Figures 6 and 7. These parameters have a significant contribution in this case near and at the threshold. Moreover, it can be seen that the squeeze parameter produces a more bright light than the parametric amplifier. The maximum degree of entanglement and squeezing also occurs not very far from the threshold at which an intense light is produced by manipulation of the amplitude of the parametric amplifier and squeeze parameter. On the contrary, as the amplitude of the driving radiation becomes stronger, the intensity of the light becomes lesser.

6.2. Photon Number Fluctuation. Here, we study the variance in the photon number for the cavity light. The variance

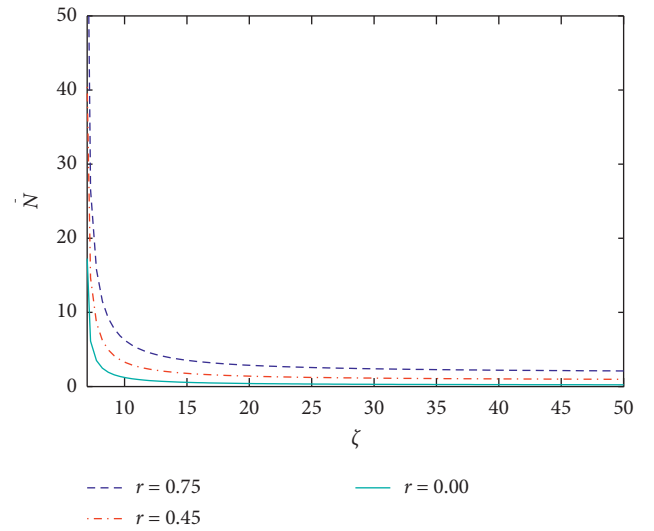


FIGURE 7: Plots of the steady state mean photon number (equation (57)) versus ζ for $\kappa = 0.8$, $\varepsilon = 0.20$, and $A = 2.50$ and for different values of r .

of the photon number is one of the features categorizing a light source exhibiting quantum and classical properties [35]:

$$\Delta N^2 = \langle (\hat{c}^\dagger \hat{c})^2 \rangle - \langle \hat{c}^\dagger \hat{c} \rangle^2. \quad (58)$$

Equation (58) can be rewritten, by making use of the bosonic commutation relation $[\hat{c}, \hat{c}^\dagger] = 1$, in the form

$$\Delta N^2 = \langle \hat{c}^{\dagger 2} \hat{c}^2 \rangle + \langle \hat{c}^\dagger \hat{c}^2 \rangle - \langle \hat{c}^\dagger \hat{c} \rangle^2. \quad (59)$$

It is realized that α and β are Gaussian variables with zero mean. Thus, in terms of the c -number variables associated with the normal ordering, it is not difficult to find that

$$\Delta N^2 = \langle \alpha \beta \rangle^2 + \bar{N}(1 + \bar{N}). \quad (60)$$

The result presented in equation (60) indicates that the variance of the photon number is greater than the mean photon number of the cavity radiation $\Delta N^2 > \bar{N}$. Consequently, the cavity light exhibits super-Poissonian photon statistics for all cases while exhibiting nonclassical properties in various conditions.

6.3. Photon Number Correlation. In this section, we analyze the photon number correlation of the cavity radiation. Nonclassical features of the radiation are usually studied via the amplification of the correlation in the quadrature operators. In many instances, experimental realization of the theoretical prediction in this line has been found to be a formidable task due to the complication involved in the homodyne and phase measurements. Thus, an alternative approach for studying the quantum features of the cavity radiation which involves simultaneous photon count measurement is required. The equal time photon number correlation for light mode \hat{a} and light mode \hat{b} can be expressed as

$$g_{(\bar{n}_a, \bar{n}_b, \bar{n}_{ab})}^{(2)}(0) = \frac{\langle \hat{a}^\dagger \hat{b}^\dagger \hat{a} \hat{b} \rangle}{\langle \hat{a}^\dagger \hat{a} \rangle \langle \hat{b}^\dagger \hat{b} \rangle}. \quad (61)$$

In view of the fact that the separate cavity-mode variables are c -number Gaussian variables of vanishing mean, we find that

$$g_{(\bar{n}_a, \bar{n}_b, \bar{n}_{ab})}^{(2)}(0) = 1 + \frac{\langle \alpha \beta \rangle^2}{\langle \alpha^* \alpha \rangle \langle \beta^* \beta \rangle}. \quad (62)$$

This equation describes equal time steady state photon number correlation of a two-mode cavity radiation. In the following, we investigate the explicit dependence of the steady state photon number correlation on the amplitude of the parametric amplifier and squeeze parameter.

Figure 8 explicitly presents that the photon number correlation grows with decreasing the amplitude of the parametric amplifier. It is also possible to realize that the mean photon number correlation grows fast with the amplitude of the classical driving radiation at the threshold but slowly increases far from the threshold. The entanglement and squeezing properties of the cavity radiation are also observed to be enhanced almost sharply in the region where the photon number correlation grows fast with amplitude of the classical pumping. Moreover, it is observed that $g_{(\bar{n}_a, \bar{n}_b, \bar{n}_{ab})}^{(2)}(0) > 2$ showing that the cavity radiation is entangled and described by Gaussian variables of vanishing mean [33, 35]. The squeeze parameter plays in the same way as the parametric amplifier on the variation of the photon number correlation as it can be seen in Figure 9. Moreover, it is clearly evident that the variation in photon number correlation due to varying r from 0.45 to 0.75 is smaller compared to the variation of r from 0 to 0.45. In this light, the photon number correlation can be used, similar to the squeezing and entanglement, in demonstrating the effect of the external environment that dominates the cavity light

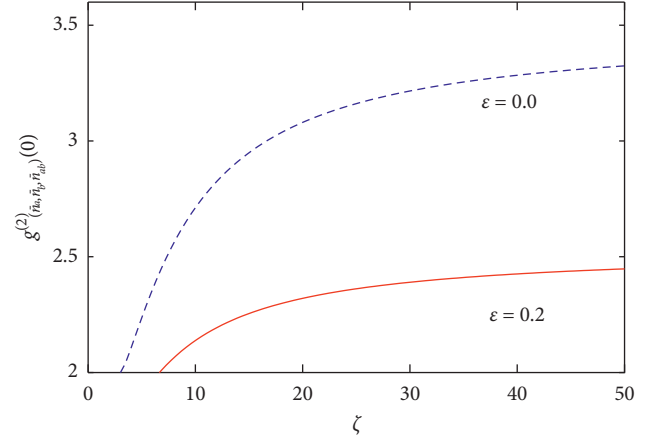


FIGURE 8: Plots of the steady state photon number correlation (equation (62)) versus ζ for $\kappa = 0.8$, $r = 0.75$, and $A = 2.50$ and for different values of ϵ .

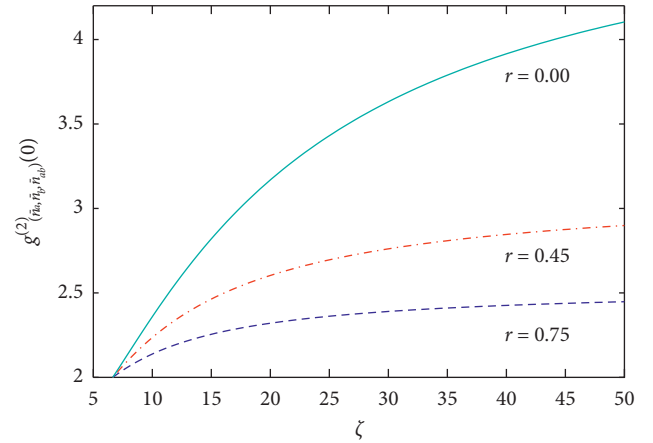


FIGURE 9: Plots of the steady state photon number correlation (equation (62)) versus ζ for $\kappa = 0.8$, $\epsilon = 0.20$, and $A = 2.50$ and for different values of r .

when r is larger, 0.75 in this case. Moreover, it can be seen from Figures 8 and 9 that the correlation between the photon numbers tends to be minimum in the regions where the squeezing and entanglement are maximum. This is due to the fact that the mean photon number of the separate cavity modes, which are inversely related to the photon number correlation, is large.

6.4. Intensity Difference Fluctuation. In this section, the intensity difference fluctuation of the cavity radiation is studied. This study is based on the assumption that there is a difference between the mean photon numbers of the two radiations due to the disparity of the absorption emission mechanism among the involved atomic energy levels. The intensity difference fluctuation allows us to investigate how the difference between the mean photon numbers of the two radiations deviates from each other. Therefore, the fluctuation of the intensity difference can be defined as

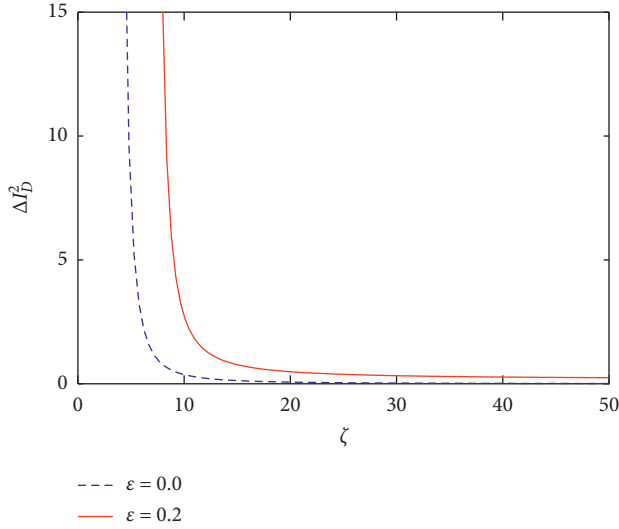


FIGURE 10: Plots of the steady state intensity difference fluctuation (equation (64)) versus ζ for $\kappa = 0.8$, $r = 0.75$, and $A = 2.50$ and for different values of ϵ .

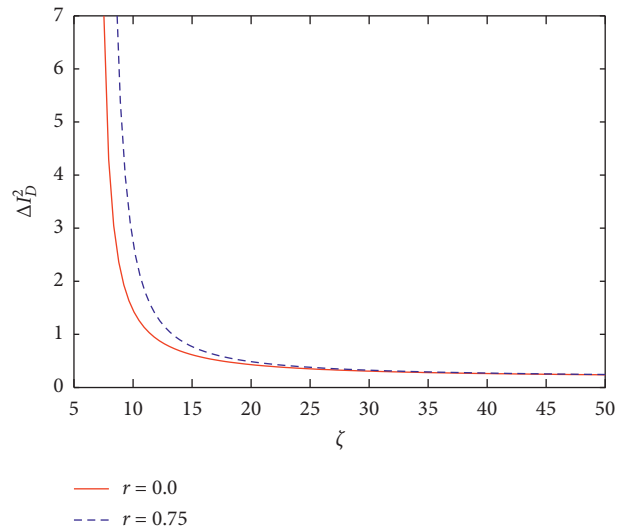


FIGURE 11: Plots of the steady state intensity difference fluctuation (equation (64)) versus ζ for $\kappa = 0.8$, $\epsilon = 0.20$, and $A = 2.50$ and for different values of r .

$$\Delta I_D^2(t) = \langle \hat{I}_D^2(t) \rangle - \langle \hat{I}_D(t) \rangle^2, \quad (63)$$

in which $\hat{I}_D = \hat{a}^\dagger(t)\hat{a} - \hat{b}^\dagger(t)\hat{b}(t)$ is the intensity difference. Taking into account properties pertaining to Gaussian variables [35], it can be verified that

$$\Delta I_D^2 = \langle \alpha^* \alpha \rangle [1 + \langle \alpha^* \alpha \rangle] + \langle \beta^* \beta \rangle \times [1 + \langle \beta^* \beta \rangle] - 2\langle \alpha \beta \rangle^2. \quad (64)$$

We then investigate the explicit dependence of the intensity difference fluctuation on the amplitude of the parametric amplifier and squeeze parameter.

It is not subtle to see from Figures 10 and 11 that the fluctuation of the intensity difference increases with the

amplitude of the parametric amplifier and the squeeze parameter. The influence of the parametric amplifier is more prominent at the threshold while the effect of the squeeze parameter is insignificant in enhancing the intensity difference fluctuation altogether in particular in the strong driving field. However, unlike the photon number correlation, it declines with the amplitude of the classical pumping far away from the threshold. Moreover, the variance of the intensity difference is found to be larger at the threshold for which the mean photon number is also larger.

7. Conclusion

In this paper, the quantum statistical properties of the two-mode cavity light, which is generated by a correlated emission laser with a nondegenerate parametric amplifier and coupled to the squeezed vacuum reservoir, have been investigated. First, the master equation in the good cavity limit, linear, and adiabatic approximation schemes has been determined. Applying the stochastic master equation, the equations of evolution of the first and second moments of the cavity-mode variables have been derived. With the aid of these equations, the quadrature fluctuations, smallest eigenvalue of the symplectic matrix, mean photon number, photon number fluctuation, photon number correlation, and intensity difference fluctuation of the cavity radiation are obtained. Then, the quantum statistical properties of the cavity light have been analyzed varying the parameters involved in the system.

A robust squeezed and entangled light of 91% have been produced by manipulating the parameters involved in this quantum optical device. The amount of squeezing and entanglement produced by this system is by far stronger than the one generated by another devices, for example, correlated emission laser with a maximum atomic coherence and coupled with the vacuum reservoir in the absence [10] and presence [21, 33] of the nonlinear crystal. Therefore, the atomic correlation induced among the emitted photons by the classical pumping radiation along with the parametric amplifier and squeezed vacuum reservoir leads to a significant enhancement of the squeezing and entanglement properties of the cavity light.

Besides, a quite robust intensity of the cavity radiation has also been demonstrated upon manipulating the parameters that has enhanced the squeezing and entanglement in the proposed scheme. The photon number correlation, similar to the squeezing and entanglement, has correctly demonstrated the effect of the huge external environment that dominates the small cavity system. The correlation between the photon numbers tends to be minimum in regions where the squeezing and entanglement are maximum due to the fact that the mean photon number of the separate cavity modes is inversely related to the photon number correlation. Furthermore, the intensity difference fluctuation increases with the amplitude of the parametric amplifier and squeeze parameter, and it is almost vanished in the absence of these parameters. The system also falls to the category of super-Poissonian photon statistics for all cases while exhibiting the various nonclassical properties of the

generated radiation. In general, it can be concluded that a correlated emission laser can be a promising optical device which produces a strong and bright squeezed and entangled cavity light with a rich varieties of statistical properties.

Data Availability

The data used to support the findings of this study are included within the article.

Conflicts of Interest

The authors declare that they have no conflicts of interest.

References

- [1] S. Qamar, M. Al-Amri, and M. Suhail Zubairy, "Erratum: entanglement in a bright light source via Raman-driven coherence," *Physical Review A*, vol. 79, no. 3, Article ID 013831, 2009.
- [2] J. Anwar and M. S. Zubairy, "Quantum-statistical properties of noise in a phase-sensitive linear amplifier," *Physical Review A*, vol. 49, no. 1, pp. 481–484, 1994.
- [3] N. A. Ansari, J. Zubairy, and M. S. Zubairy, "Phase-sensitive amplification in a three-level atomic system," *Physical Review A*, vol. 41, no. 9, pp. 5179–5186, 1990.
- [4] A. Mortezaipoor, M. Mahmoudi, and M. R. H. Khajepour, "Atom-photon, two-mode entanglement and two-mode squeezing in the presence of cross-Kerr nonlinearity," *Optical and Quantum Electronics*, vol. 47, no. 7, pp. 2311–2329, 2015.
- [5] C. A. Blockley and D. F. Walls, "Intensity fluctuations in a frequency down-conversion process with three-level atoms," *Physical Review A*, vol. 43, no. 9, pp. 5049–5056, 1991.
- [6] N. Lu, F.-X. Zhao, and J. Bergou, "Nonlinear theory of a two-photon correlated-spontaneous-emission laser: a coherently pumped two-level-two-photon laser," *Physical Review A*, vol. 39, no. 10, pp. 5189–5208, 1989.
- [7] T. Abebe, N. Gemechu, C. Gashu, K. Shogile, S. Hailemariam, and Sh. Adisu, "The quantum analysis of nonlinear optical parametric processes with thermal reservoirs," *International Journal of Optics*, vol. 2020, Article ID 7198091, 11 pages, 2020.
- [8] C. G. Feyisa and T. Abebe, "Externally induced entanglement amplification in a coherently pumped emission of laser with parametric amplifier and coupled to squeezed vacuum reservoir," *Physica Scripta*, vol. 95, no. 7, Article ID 075105, 2020.
- [9] S. Tesfa, "Effects of decoherence on entanglement in a correlated emission laser," *Journal of Physics B: Atomic, Molecular and Optical Physics*, vol. 40, no. 12, pp. 2373–2384, 2007.
- [10] S. Tesfa, "Entanglement amplification in a nondegenerate three-level cascade laser," *Physical Review A*, vol. 74, Article ID 043816, 2006.
- [11] T. Abebe and N. Gemechu, "Two-level atom with squeezed light from optical parametric oscillators," *Ukrainian Journal of Physics*, vol. 63, no. 7, p. 600, 2018.
- [12] R. Vyas and S. Singh, "Photon-counting statistics of the degenerate optical parametric oscillator," *Physical Review A*, vol. 40, no. 9, pp. 5147–5159, 1989.
- [13] L. I. Plimak and D. F. Walls, "Dynamical restrictions to squeezing in a degenerate optical parametric oscillator," *Physical Review A*, vol. 50, no. 3, pp. 2627–2641, 1994.
- [14] K. Fesseha, "Parametric oscillation with a squeezed vacuum," *Optics Communications*, vol. 156, no. 1–3, pp. 145–157, 1998.
- [15] R. T. Glasser, H. Cable, J. P. Dowling, F. De Martini, F. Sciarrino, and C. Vitelli, "Entanglement-seeded, dual, optical parametric amplification: applications to quantum imaging and metrology," *Physical Review A*, vol. 78, no. 1, Article ID 012339, 2008.
- [16] L. A. Lugiato and G. Strini, "On the squeezing obtainable in parametric oscillators and bistable absorption," *Optics Communications*, vol. 41, no. 1, pp. 67–70, 1982.
- [17] G. Milburn and D. F. Walls, "Production of squeezed states in a degenerate parametric amplifier," *Optics Communications*, vol. 39, no. 6, pp. 401–404, 1981.
- [18] P. D. Drummond, K. Dechoum, and S. Chaturvedi, "Critical quantum fluctuations in the degenerate parametric oscillator," *Physical Review A*, vol. 65, no. 3, Article ID 033806, 2002.
- [19] M. D. Reid and P. D. Drummond, "Quantum correlations of phase in nondegenerate parametric oscillation," *Physical Review Letters*, vol. 60, no. 26, pp. 2731–2733, 1988.
- [20] Z. Y. Ou, S. F. Pereira, H. J. Kimble, and K. C. Peng, "Realization of the Einstein-Podolsky-Rosen paradox for continuous variables," *Physical Review Letters*, vol. 68, no. 25, pp. 3663–3666, 1992.
- [21] T. Abebe, N. Gemechu, K. Shogile, S. Hailemariam, C. Gashu, and S. Adisu, "Entanglement quantification using various inseparability," *Romanian Journal of Physics*, vol. 65, p. 107, 2020.
- [22] B. Daniel and K. Fesseha, "The propagator formulation of the degenerate parametric oscillator," *Optics Communications*, vol. 151, no. 4–6, pp. 384–394, 1998.
- [23] B. Teklu, "Parametric oscillation with the cavity mode driven by coherent light and coupled to a squeezed vacuum reservoir," *Optics Communications*, vol. 261, no. 2, pp. 310–321, 2006.
- [24] N. Geoffery, *Introduction to Nonlinear Optics*, Cambridge University Press, New York, NY, USA, 2011.
- [25] N. Treps, U. Andersen, B. Buchler et al., "Surpassing the standard quantum limit for optical imaging using nonclassical multimode light," *Physical Review Letters*, vol. 88, no. 20, Article ID 203601, 2002.
- [26] M. A. Taylor, J. Janousek, V. Daria et al., "Biological measurement beyond the quantum limit," *Nature Photonics*, vol. 7, no. 3, pp. 229–233, 2013.
- [27] K. Heshami, D. G. England, P. C. Humphreys et al., "Quantum memories: emerging applications and recent advances," *Journal of Modern Optics*, vol. 63, no. 20, pp. 2005–2028, 2016.
- [28] C. H. Bennett and D. P. DiVincenzo, "Quantum information and computation," *Nature*, vol. 404, no. 6775, pp. 247–255, 2000.
- [29] S. Barzanjeh, S. Pirandola, and C. Weedbrook, "Continuous-variable dense coding by optomechanical cavities," *Physical Review A*, vol. 88, no. 4, Article ID 042331, 2013.
- [30] J.-G. Ren, P. Xu, H.-L. Yong et al., "Ground-to-satellite quantum teleportation," *Nature*, vol. 549, no. 7670, pp. 70–73, 2017.
- [31] C. L. Degen, F. Reinhard, and P. Cappellaro, "Quantum sensing," *Reviews of Modern Physics*, vol. 89, no. 3, Article ID 035002, 2017.
- [32] C. G. Feyisa, "Enhanced CV entanglement quantification in a CEL with parametric amplifier and coupled to squeezed vacuum," *Brazilian Journal of Physics*, vol. 50, no. 4, pp. 379–393, 2020.
- [33] C. Gashu, E. Mosisa, and T. Abebe, "Entanglement quantification of correlated photons generated by three-level laser with parametric amplifier and coupled to a two-mode vacuum

- reservoir,” *Advances in Mathematical Physics*, vol. 2020, Article ID 9027480, 14 pages, 2020.
- [34] S. Tesfa, “Continuous variable entanglement in a coherently pumped correlated emission laser,” *Journal of Physics B: Atomic, Molecular and Optical Physics*, vol. 41, Article ID 055503, 2008.
- [35] K. Fesseha, *Fundamental of Quantum Optics*, Lulu, Durham, NC, USA, 2008.
- [36] T. Abebe and C. G. Feyisa, “Dynamics of a nondegenerate three-level laser with parametric amplifier and coupled to a two-mode squeezed vacuum reservoir,” *Brazilian Journal of Physics*, vol. 50, pp. 495–508, 2020.
- [37] G. Adesso, A. Serafini, and F. Illuminati, “Extremal entanglement and mixedness in continuous variable systems,” *Physical Review A*, vol. 70, no. 2, Article ID 022318, 2004.
- [38] G. Vidal and R. F. Werner, “Computable measure of entanglement,” *Physical Review A*, vol. 65, no. 3, Article ID 032314, 2002.